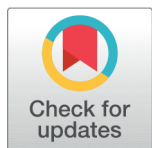


RESEARCH ARTICLE

 OPEN ACCESS

Received: 23-04-2020

Accepted: 14-06-2020

Published: 23-06-2020

Editor: Dr. Natarajan Gajendran

Citation: Kumar R, Kumar G, Kumar M, Guleria RP (2020) Spectral and seasonal variations of aerosol optical depth with special reference to Kanpur, Indo-Gangetic Basin. Indian Journal of Science and Technology 13(21): 2119-2137. <https://doi.org/10.17485/IJST/v13i21.364>

*Corresponding author.

Gulshan Kumar

Department of Physics, Govt. College Sarkaghat, District Mandi, 175024, Himachal Pradesh, India. Tel.: +919418195031
goldy_physics@rediffmail.com

Funding: None

Competing Interests: None

Copyright: © 2020 Kumar, Kumar, Kumar, Guleria. This is an open access article distributed under the terms of the [Creative Commons Attribution License](https://creativecommons.org/licenses/by/4.0/), which permits unrestricted use, distribution, and reproduction in any medium, provided the original author and source are credited.

Published By Indian Society for Education and Environment ([iSee](https://www.indjst.org/))

Spectral and seasonal variations of aerosol optical depth with special reference to Kanpur, Indo-Gangetic Basin

Raj Kumar^{1,2}, Gulshan Kumar^{3*}, Mukesh Kumar⁴, Raj Paul Guleria⁵¹ Department of Physics, Career Point University Kota, Kota, 324005, Rajasthan, India² Department of Physics, Govt. College Ghumarwin, District Bilaspur, 174021, Himachal Pradesh, India³ Department of Physics, Govt. College Sarkaghat, District Mandi, 175024, Himachal Pradesh, India. Tel.: +919418195031⁴ Department of Physics, Lovely Professional University, Phagwara, 144411, Punjab, India⁵ Department of Higher Education, Govt. Of Himachal Pradesh, 171001, Himachal Pradesh, India

Abstract

Objectives: To find characteristics of Aerosol optical depth (AOD) at ultra-violet (340-380 nm), visible (440-675 nm) and near-infrared (870-1020 nm) wavelength spectrum. During estimation of the radiative effect of aerosol in the atmosphere of earth radiation budget, it is important to study AOD. It is the total disappearance of sun rays due to aerosols in atmospheric column by absorption and scattering. **Methodology:** AOD is being measured using ground based sensor called CIMEL Sun photometer over Kanpur as it is situated in the Indo-Gangetic Basin. **Findings:** The seasonal variations in AOD as well as in various months of the year at 340nm, 500nm and 1020nm under all clear days have been studied. The observations showed that AOD was increasing from Pre-monsoon to Post-monsoon season at short wavelengths; whereas it was found to be decreasing at longer wavelengths regions. **Novelty:** Area under study is surrounded by small to large scale industries. Therefore, industrial emission is a major source of anthropogenic aerosols. The study of spectral and seasonal variations of Aerosol Optical Depth is important because the accumulation of aerosol particularly mixing state of aerosols has impact on atmospheric dynamics. Furthermore this work will also motivate the researchers to develop aerosol climatology map particularly for Indian regions.

Keywords: Aerosol optical depth (AOD); CIMEL sun photometer; solar radiations

1 Introduction

The small sized particles drifting between surface of earth and stratosphere (in solid, liquid or gaseous phase) are called Atmospheric aerosols⁽¹⁾. These particles are created in the atmosphere or transported to the atmosphere by various sources.⁽²⁻⁴⁾ These aerosols may be primary or secondary. Primary aerosols are released directly through atmosphere while secondary aerosols are created in the atmosphere from precursor gases^(5,6). The origins of primary aerosols are partial combustion of fossil fuels, burning of biomass, mineral particles sea spray, volcanic eruptions, etc.^(1-3,6). The main components of secondary aerosols are sulphate and nitrate⁽⁴⁻⁶⁾. These are categorized as fine-mode (radius < 0.1 μm), accumulation-mode (0.1 $\mu\text{m} \leq$ radius < 1.0 μm) and coarse mode (radius \geq 1.0 μm) aerosols⁽⁵⁾. The composition, structure and the size of the particle changes with various atmospheric processes like coagulation, dry deposition, evaporation and convection⁽⁶⁾. During atmospheric transport, aerosol particles undergo diffusion possibly by collision in turbulent and Brownian processes. The process of coagulation happens due to the collision among these particles. This process often increases the concentration of larger particles and simultaneously decreases the smaller particles. During their lifecycle, particles are appeared to be changed by such processes.

There is a strong interaction between aerosols and solar radiations which cause a great effect on climate change⁽⁷⁾. So the radiative balance of earth is influenced^(7,8). It alters hydrological cycle, effects weather and influences major monsoons of the world⁽⁹⁻¹²⁾. However it is rare to say whether aerosol influences the cooling or heating of environment^(7,8). Due to different processes there is an alarming increase in load of aerosols in atmosphere with big threat to the world⁽¹⁰⁻¹²⁾. This threat attracts the worldwide researchers to get ample researches in this context. The some of the basic factors which affect the radiative effects of aerosol particles are single scattering albedo (SSA, ω), aerosol optical depth (AOD, $\tau_{p\lambda}$), asymmetry factor (Assy, g), surface albedo, concentration of aerosols, composition, their size and structure⁽⁷⁾. Their spatial and temporal variations are of paramount importance may be due to diversified source origins⁽²⁻⁵⁾ (13-16).

The Indian subcontinent comprised of inland plains, mountains, semiarid areas, coastal and plateau areas and experience tropical and subtropical climatic conditions. The uneven heating of earth's surface by sun radiation results in temperature gradient in the atmosphere which forces the atmosphere into motion and thereby plays a vital participation in influencing and regulating the spatial-temporal variability in the features of aerosol⁽¹⁷⁻¹⁹⁾. Source of such data is National Centre for Environment Prediction (NCEP). The climate variables over Indian regions are average vector wind designs, velocity of wind, relative humidity, air temperature, and condensation rates in different seasons. The highest wind speed on the surface is normally found higher during pre-monsoon period, with a surface wind observed at more than 2 ms^{-1} in comparison to its normal speed (<2.0 ms^{-1}). During monsoon, relative humidity is noticed greatest (above 70%) and smallest during winter (55%). During all season large variation in latitudinal temperature is observed. This latitudinal temperature variation is more pronounced in pre-monsoon season. Monsoon season is the season when Indian region receive maximum precipitation.

The AERONET is an extensive ground-based remote sensing aerosol world-wide network, the CIMEL sun/sky spectral radiometers are installed at different locations of the globe. In India, this instrument became operational on January 22, 2001 after the agreement signed between IIT Kanpur and NASA and since then providing high-quality data to public domain, which is used by the Indian as well as international scientists to analyze the optical features of aerosols and their impact on radiative forcing. The CIMEL sun/sky spectral radiometer has been designed to make spectral measurements of solar radiation

extinction studies at ultra-violet, visible and near infrared wavelengths. AERONET delivers constant data of AOD and outcomes of inversion aerosols in various aerosols areas. The data taken from SUNY radiation model for the period 2002-2008 showed the low value of direct irradiance in hazy area but high value in Himalayas where AOD is remarkably lesser⁽²⁰⁾. The observations of aerosol optical characteristics by AERONET installed at Gandhi College and Kanpur indicate a remarkable spatial comparison in the properties of aerosols amid eastern and central Indo-Gangetic Basin⁽²¹⁾. The study of spectral and seasonal variations of Aerosol Optical Depth from this part of India is important because the accumulation of aerosol particularly mixing state of aerosols has impact on atmospheric dynamics. This work will motivate the researchers to develop aerosol climatology map particularly for Indian regions and to monitor aerosols in different geographical regions This paper aims to find the characteristics of AOD at ultra-violet (340-380 nm), visible (440-675 nm) and near-infrared (870-1020 nm) wavelength spectrum using ground based sensor called CIMEL sun photometer over Kanpur as it is located in the Indo-Gangetic Basin (IGB).

2 Study Area

The work has been conducted to present regional aerosol characteristics and underlying aerosol transport process using application of ground-based observations. The data in the present paper has been collected from CIMEL sun photometer, which is situated in the campus of the IIT Kanpur (26.51°N, 80.23°E; 123 m amsl; period: 2001-2015) under AERONET programme (Source: <http://aeronet.gsfc.nasa.gov>).

Kanpur is situated in the Indo-Gangetic Basin (IGB) and is considered as an industrialized urban location⁽²²⁾. This site is surrounded by small to large scale industries where, industrial emission is a major source of anthropogenic aerosols⁽²³⁾. The synoptic wind pattern is observed from northwest to southwest⁽²⁴⁾. The daily AOD retrieved by the MODIS Terra at the Indo-Gangetic Basin stations is also found in good agreement with the AERONET measured AOD⁽²⁵⁾. The continuous measurements of direct sun rays intensities arriving the surface of this region have also been done for long time.

3 Methodology

CIMEL sun photometer is an automatic instrument which runs without any operator assistance. During sunrise its collimator is pointed towards the solar disc. The filter wheel rotates in sequence order to make spectral solar radiation extinction measurements at an interval of 10 seconds. To characterize the presence of slim wispy clouds, which can be irregular, three measures of concatenation are carried out, which keep going approximately 35 seconds. The measurements of direct solar irradiance are in sequence wise order by the filter wheel assembly at every 0.5air-mass above an air-mass of 2 and, in any case, each 15 minutes. The data of the almucantar sun (radiation at a constant angle of the sun's zenith) is received twice a day (depending upon weather conditions) at an angle of the sun's zenith of about 60 degrees in four channels: 440, 670, 870 and 1020 nm, whereas the sky radiance of the main solar plane is received four times a day on these channels. Observations on zenith radiation in cloud mode are obtained at regular interlude between the observation-planes indicated above (if it may not rain). Whole records are saved in the control field of the CIMEL solar photometer. The PC instrument receives data from the control unit within a few hours and transfers it to AERONET for next rectification.

The AERONET is a worldwide sun photometer network (<http://aeronet.gsfc.nasa.gov>) for measuring the aerosol optical properties. The associates of national establishments, organizations, universities, individual researchers and partners have significantly extended the AERONET program. The program gives a lasting and easily accessible publicly available database on the optical, microbiological and radiative prop-

erties of aerosols for the study and characterization of aerosols, validation of satellite studies and synergies with other databases. The network is known for standardizing, calibrating, processing and disseminating data. The network gives data on aerosol optical properties such as AOD, single scattering albedo (SSA) and aerosol size distribution (ASD).

AERONET provides worldwide observations of the optical properties of aerosols in different aerosol modes, with high temporal resolution and three levels of data quality: level 1.0 (unshielded), level 1.5 (cloud screened) and level 2.0 (cloud screened and quality assurance)⁽²⁶⁾. Owing to its high precision (accuracy: ± 0.01), long working history and global reach, the data of AERONET data has been utilized as a reference level for AOD measurement and model validation of many aerosol sensors^(2,26). The level 2.0 daily average monthly aerosol products have been used in this study.

This instrument is designed according to the principle described in Shaw et al. (1973). Usually, direct sunlight is obtained during large air mass periods at 0.25 mass intervals while in smaller air masses; the time between measurements is 15 minutes. The optical depth is calculated from the spectral extinction of the direct radiation at each wavelength according to Beer-Lambert-Bouguer's law:

$$E_{\lambda} = E_{oi} \left(\frac{d_m}{d} \right)^2 \exp(-m\tau_{\lambda})$$

where E_{λ} is the surface reaching solar radiation and, in the case of the CIMEL solar photometer, is the signal measured from the instrument. $E_{o\lambda}$ is the incident solar radiation at the top of the atmosphere and, in the case of the CIMEL sun photometer, is the extraterrestrial signal (calibration constant) of the instrument. $E_{o\lambda}$ is obtained according to the average earth-sun distance ' d_m ', d is the distance on the day of observation, m is the optical air mass which is a function of the angle of the solar zenith (SZA, z) and τ_{λ} is the total columnar optical column.

The correction of earth-sun distance called eccentricity correction factor is computed by taking into account the approximation:

$$\left(\frac{d_m}{d} \right)^2 = 1 + 0.034 \cos \frac{2\pi J}{365}$$

where J is the total days in the year⁽²⁷⁾. The optical air-mass m is a function of the zenith angle z of the sun and is found as:

$$m = \left\{ \cos \frac{\pi}{180^\circ} + 0.15 \times (93.885 - z)^{-1.253} \right\}^{-1}$$

The raw data obtained by CIMEL sun photometer is reanalyzed to obtain AOD (τ_{λ}) on the log scale according to Langley techniques by taking a linear regression fit to the Lambert-Beer Law⁽²⁸⁾.

$$\ln E_{\lambda} = \ln E_{o\lambda} + 2 \ln \left(\frac{d_m}{d} \right) - m\tau_{\lambda}$$

We get the total columnar optical depth (τ_{λ}) as a result of distinct atmospheric extinction processes such as scattering by air molecules ($\tau_{r\lambda}$), aerosols ($\tau_{p\lambda}$) and absorption due to gaseous and water vapor ($\tau_{\alpha\lambda}$) consisting $\tau_{o\lambda}$ and $\tau_{w\lambda}$; which are represented as:

$$\tau_{\lambda} = \tau_{r\lambda} + \tau_{\alpha\lambda} + \tau_{p\lambda}$$

The inversion algorithm also used to restore: (1) spectral characteristics of columnar aerosol which incorporates aerosol optical depth, single scattering albedo and phase function (2) aerosol size distribution and refractive index⁽²⁹⁾. The relationship between the two sets of aerosol parameters can be obtained in the following integrals:

$$\tau_{p, \text{ext}}(\lambda) = \frac{2\pi}{\lambda} \int_{r_{\min}}^{r_{\max}} K_{\text{ext}}(x, \mu) V(r) d \ln(r)$$

$$\beta_p(\Theta) = \frac{2\pi}{\lambda} \int_{r_{\min}}^{r_{\max}} K(\Theta, x, \mu) V(r) d \ln(r)$$

where, $\beta_p(\Theta)$ represents the single scattering component, x is the size parameter determined by $2\pi r/\lambda$, μ is the aerosol complex refractive index of aerosol, Θ is scattering angle, $V(r)$ is the columnar aerosol volume distribution, r_{\min} and r_{\max} are the minimum and maximum values of aerosol radii respectively. $K_{\text{ext}}(x, \mu)$ and $K(\Theta, x, \mu)$ are the kernel functions defined by:

$$K_{\text{ext}}(x, \mu) = \frac{3}{4} \frac{Q_{\text{ext}}(x)}{x}$$

$$K(\Theta, x, \mu) = \frac{3}{2} \frac{i_1 + i_2}{x^3}$$

Where, Q_{ext} represents the extinction efficiency factor whereas i_1 and i_2 are the intensity functions. Mie scattering theory (especially for spherical particles) and T-matrix method are used to find these functions^(30,31).

The phase function is the angular distribution of the intensity of light scattered by a particle at a particular wavelength. It occurs at an angle φ corresponding to the incident beam. It is an infinite series of orthogonal basis functions like Legendre polynomials:

$$P(\cos \varphi) = \sum_{i=0}^{N-1} \beta_i P_i(\cos \varphi)$$

Where β_i and $P_i(\cos \varphi)$ are the moments of the phase function and Legendre polynomials respectively.

The aerosol columnar volume size distribution can be described by using log-normal distribution:

$$\frac{dV}{d \ln R} = \frac{V_0}{\sigma \sqrt{2\pi}} \exp \left[-\frac{\ln \left(\frac{R}{R_m} \right)^2}{2\sigma^2} \right]$$

where, $dV/d \ln R$ is the size distribution of aerosol volume and V_0 is the particles volume column in unit cross sectional area of atmospheric column. R and R_m are the particle and modal radii respectively. σ refers to the standard deviation of the natural logarithm of particle radii. For particle retrieval in the size range $0.1 < r < 7 \mu\text{m}$, the error may increase up to 10% in maxima values whereas it may increase up to 35% in the minimum values⁽³²⁾. However, for the particles having sizes less than $0.1 \mu\text{m}$ or greater than $7 \mu\text{m}$, the error can be large. Further, depending on the types and loading of the aerosols, the uncertainty in SSA is

expected to have value between 0.03-0.05⁽²⁹⁾. The retrieved parameters should be used when solar zenith angle ≥ 50 and AOD ≥ 0.5 because in low aerosol loading conditions corresponding to small solar zenith angle the inversion-based AERONET parameters may have greater uncertainty⁽³²⁾.

Finally, a link is established between the actual radiometric measurements and the output results of the radiative transfer model (E_λ and $I_\lambda(\Theta)$). The actual radiometric outcome are the raw voltages obtained when the radiometer is directed towards the sun (direct solar component or $S(z, \varphi_o)$) and at various points of the sky (sky diffuse component or $S(z, \varphi)$). The spectral sky radiance equation at a certain number of azimuth angles is as follows

$$I_\lambda(\Theta) = Em\Delta\Omega[\omega\tau P(\Theta) + q(\Theta)]$$

where, $\Delta\Omega$ is the value of solid view angle of the radiometer, ω represents the single scattering albedo, $P(\Theta)$ refers to the phase function at scattering angle Θ , and $q(\Theta)$ the multi scattering contribution component. As for as the sky diffuse component is concerned, the radiometer is taken along the solar almucantar plane, taking the constant value of zenith angle which corresponds to solar zenith angle and the azimuthal angle (φ) is changed to obtain the values of E_λ and $I_\lambda(\Theta)$.

3.1 Uncertainties in the aerosol depth

The uncertainty in obtaining the AOD ($\tau_{p\lambda}$) results from the uncertainties in total optical depth, Rayleigh and optical depth by gas absorption. The uncertainties arises because of Rayleigh scattering by air molecules and due to ozone absorption related to wavelengths 320 and 670 nm can be ignored in comparison to the uncertainty of the total optical depth (τ_λ). Therefore, the chief uncertainty related to the total optical depth results from the uncertainty of the measured irradiance E_λ and extraterrestrial irradiance $E_{o\lambda}$ (CIMEL sun photometer calibration factor). In CIMEL sun photometer, the uncertainty related with the measured solar radiation is due to the uncertainty of calibration factor since other effects are ignored if CIMEL sun photometer operates in a proper way. The error propagation theory is used to express the absolute uncertainty in the aerosol optical depth⁽³³⁾.

$$\Delta\tau_{p\lambda} = \frac{1}{m} [\tau_{p\lambda} \Delta m + \varepsilon(E_{o\lambda}) + \varepsilon(E_\lambda)] + \frac{p}{p_o} \Delta\tau_{r\lambda} + \frac{\Delta p}{p_o} \tau_{r\lambda} + \tau_{\alpha\lambda}$$

where Δ and ε are the absolute as well as relative uncertainties respectively. The absolute uncertainty relies on m and hence changes with time. The optical air-mass ‘ m ’ changes from sunrise to sun set. The minimum value of absolute uncertainty obtained during sunrise and sunset and maximum at noon when the value of $m \approx 1$. The relative uncertainty relies on the absolute value of AOD. If we consider only the uncertainty due to measured irradiance, then uncertainty of 1% (5%) in the measured irradiance results $\Delta\tau_{p\lambda} = 0.01$ (0.05) with $m = 1$, which gives rise to relative uncertainty of 10% (50%) for a certain AOD of 0.1. For solar zenith angles $SZA < 60^\circ$, the air-mass uncertainties (Δm) may be ignored if we consider plane flat atmosphere. The uncertainty due to extraterrestrial irradiance may increase up to 1.7%⁽³⁴⁾. Thus, for air-mass $1 < m \leq 3$, the absolute uncertainty in AOD may be between ± 0.02 to ± 0.05 . AERONET considers an absolute uncertainty in the range from 0.01–0.02 for the case of CIMEL sun photometer⁽²⁶⁾.

Ideally, the outputs taken from all the datasets are differentiated at common wavelength $0.55 \mu\text{m}$. In this case, linear interpolation technique was used to calculate AERONET AOD values obtained at $0.5 \mu\text{m}$ at wavelength $0.55 \mu\text{m}$ ⁽³⁵⁾:

$$AOD_{AERONET, 550\text{nm}} = AOD_{AERONET, 500\text{nm}} \left(\frac{0.55}{0.5} \right)^{-\alpha}$$

where α is the Ångström exponent for AERONET in wavelength range between 0.44-0.87 μm and is a quantitative indicator of fine mode fraction or aerosol particle size. α is positively correlated with AOD over Kanpur⁽³⁶⁾.

4 Result and Discussion

4.1 Spectral variation of aerosol optical depth

The measurements of solar radiation extinction using CIMEL sun/sky spectral radiometer are made over Kanpur from January 2001 to November 2015. These measurements are taken during clear sky days. Number of days available for daily average AOD (Level 2.0) and contribution of day to total record (Level 2.0) are shown in Figure 1.

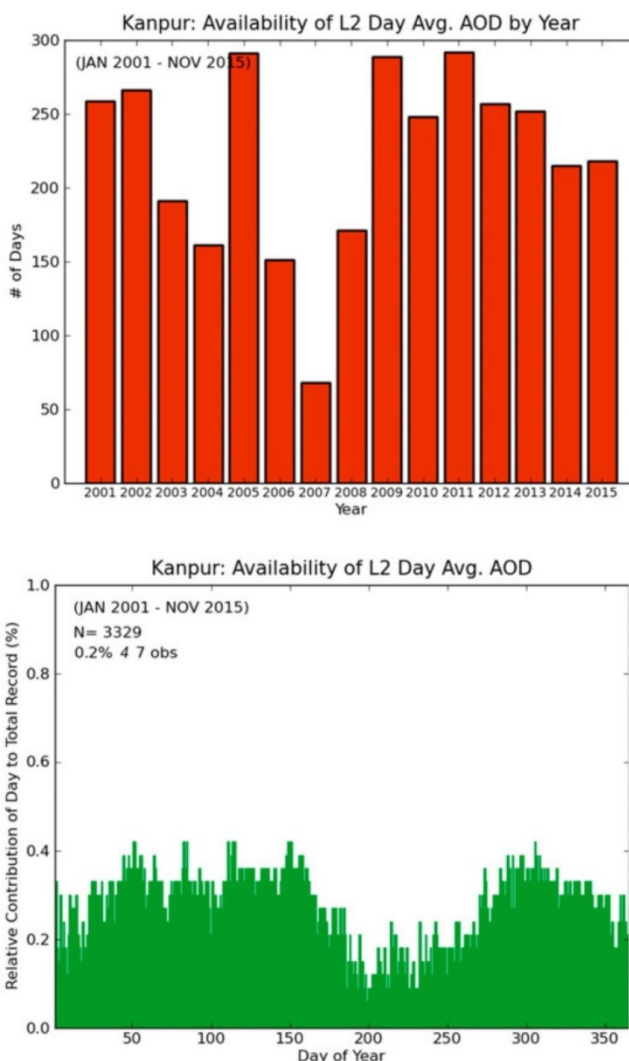


Fig 1. Average value of AODs.

Figure 2 shows the spectral variation of annual average of aerosol optical depths recorded during 2001-2015. Figure also shows the dependence of AOD on wavelength. In the figure, the vertical bars indicate

standard deviations. The standard deviations in the value of AOD are large at smaller wavelengths except in the months of June and July which shows large variations in ultra fine particles (hourly/daily basis). The AOD values are smaller during the months February - April and July - September when compared to other months of the year. The spectral slope in AOD stood different for different months of the year. The slope in AODs from March to June found rather flat, suggesting nearly independent behavior with wavelengths. A decrease in AOD with increase in wavelength i.e., specific wavelength dependent feature can be clearly observed for rest of the months (see Figure 2), that is found in good agreement with the theory of Mie scattering. These are and characteristics features of continental aerosols. The spectral properties of AOD are indicators of the spectral distribution of aerosol dimensions since they clearly show the differences between the particle sizes at distinct months⁽²⁸⁾.

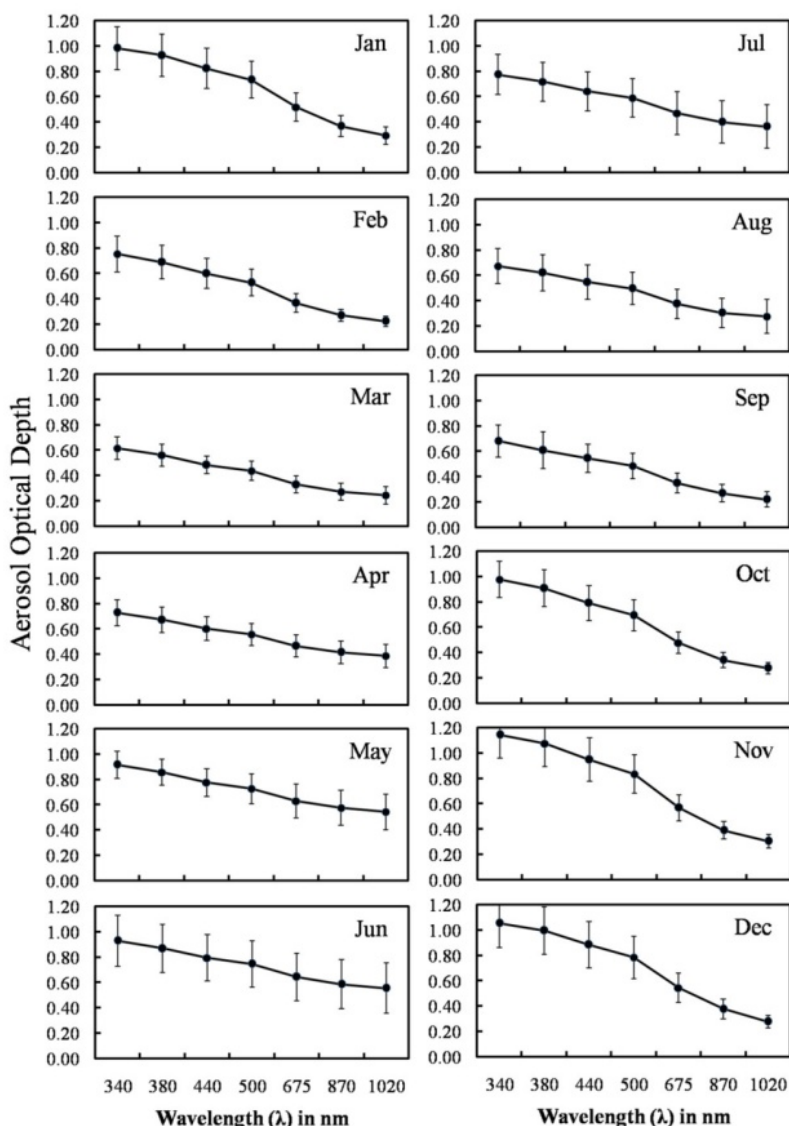
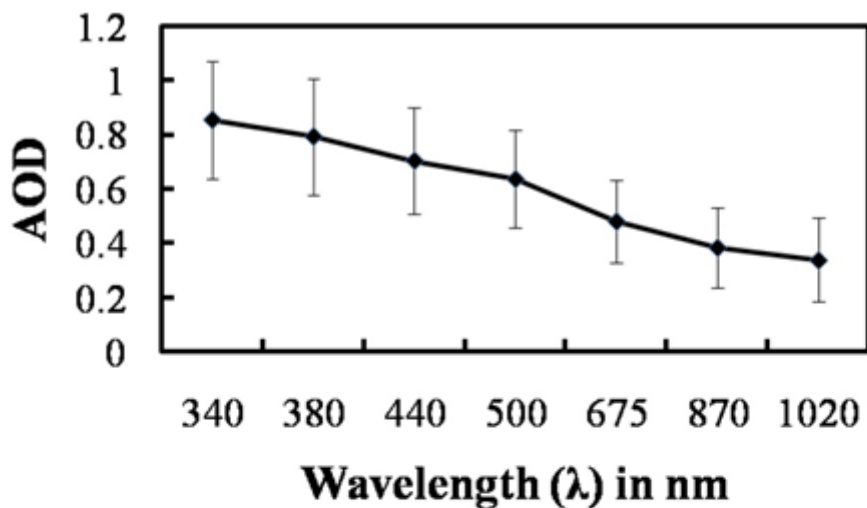
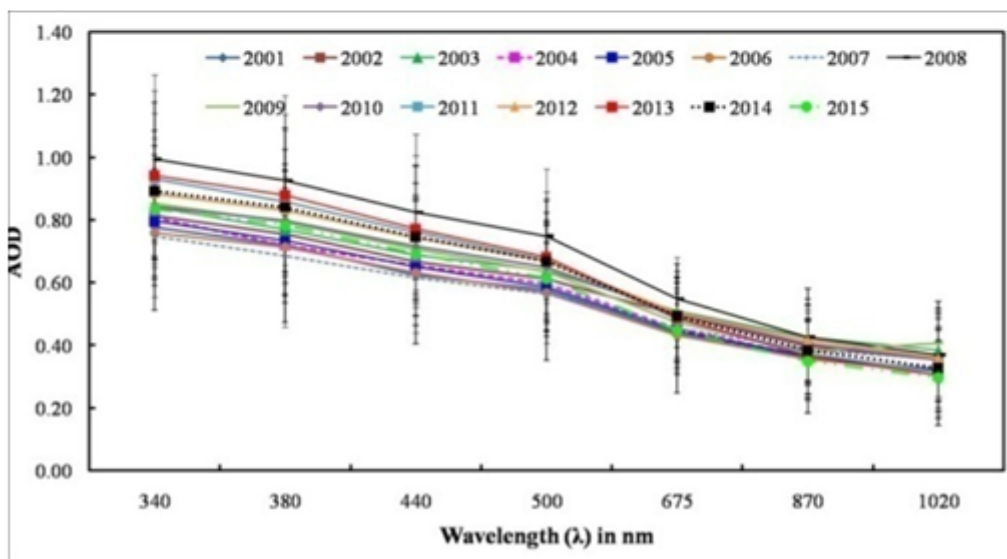


Fig 2. Annual Spectral variation of AOD over Kanpur (2001-2015), variation of AOD with wavelength (period: January 2001 to November 2015).

The monthly averaged (2001-2015) spectral variation of AOD is shown in Figure 3a. Figure 3b shows annual mean spectral AODs and its variation with wavelength. There is a gradual decrease in AOD with wavelengths which indicates a greater abundance of fine particles than coarse particles in the atmosphere⁽³⁷⁾. A slight slope at shorter wavelengths may be due to increase in production of ultra fine particles.



.(a)



.(b)

Fig 3. (a)Spectral variation in monthly average AOD, (b) annual mean spectral AODs.

Figure 4 shows the spectral variation in monthly average AOD for every year: 2001 to 2015. This figure reflects the varying characteristics of aerosol climatology in different regions. The vertical bars indicate that in 2003 the variations in aerosol properties from month to month were quit large, suggesting that

atmospheric dynamics have played a key role in modulating the aerosol properties. In general, the error bars are large at shorter wavelength, indicating a significant contribution of anthropogenic emissions. The length of error bars provides the indication about the stability of aerosol atmosphere, which can be readily noticed in 2005. The small AODs at longer wavelengths and small error bars indicating no any considerable influence of desert dust which can be readily noticed in 2015.

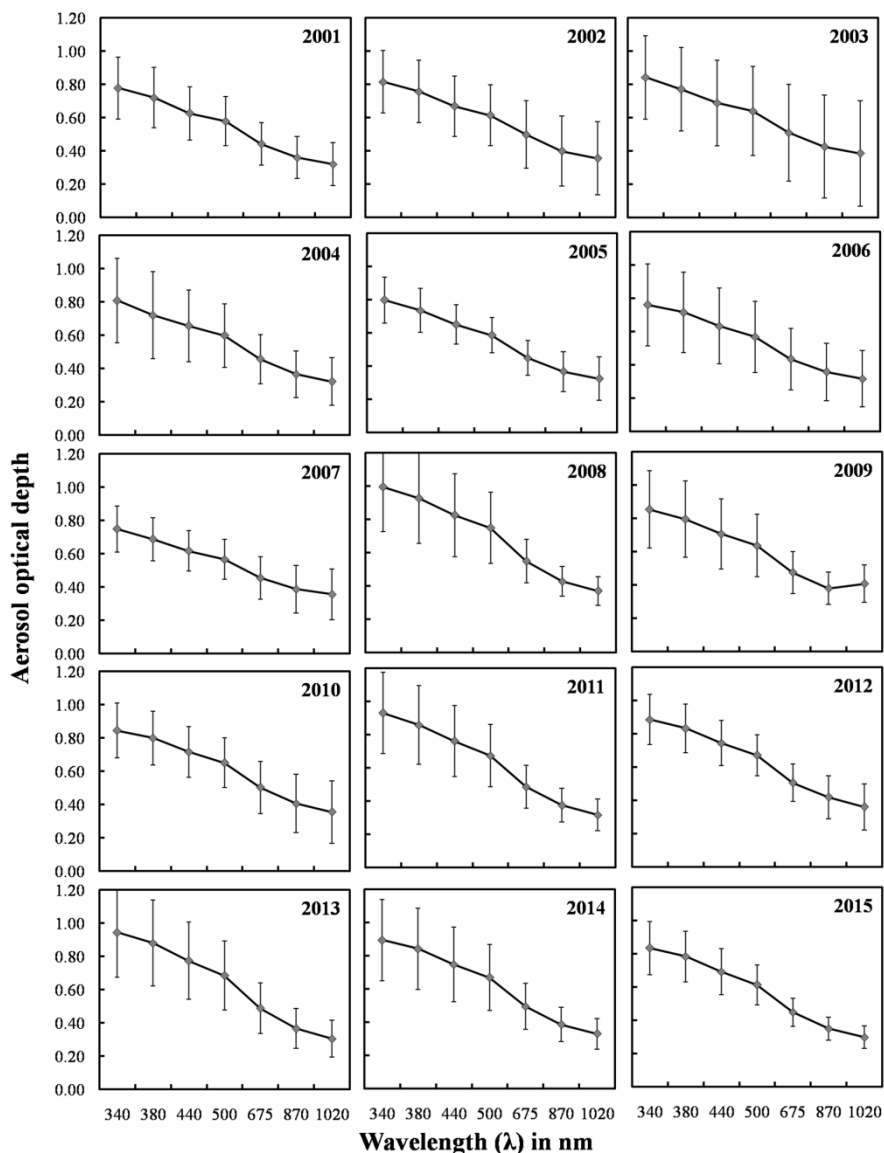


Fig 4. Spectral variation in monthly average AOD for each year from 2001 –2015. The vertical bars mentioned in the figures represent standard deviations of AOD from the mean values.

4.2 Temporal variation of aerosol optical depth

Figure 5 shows temporal (month-wise) variations of spectral AODs over the entire study period (period: 2001-2015).

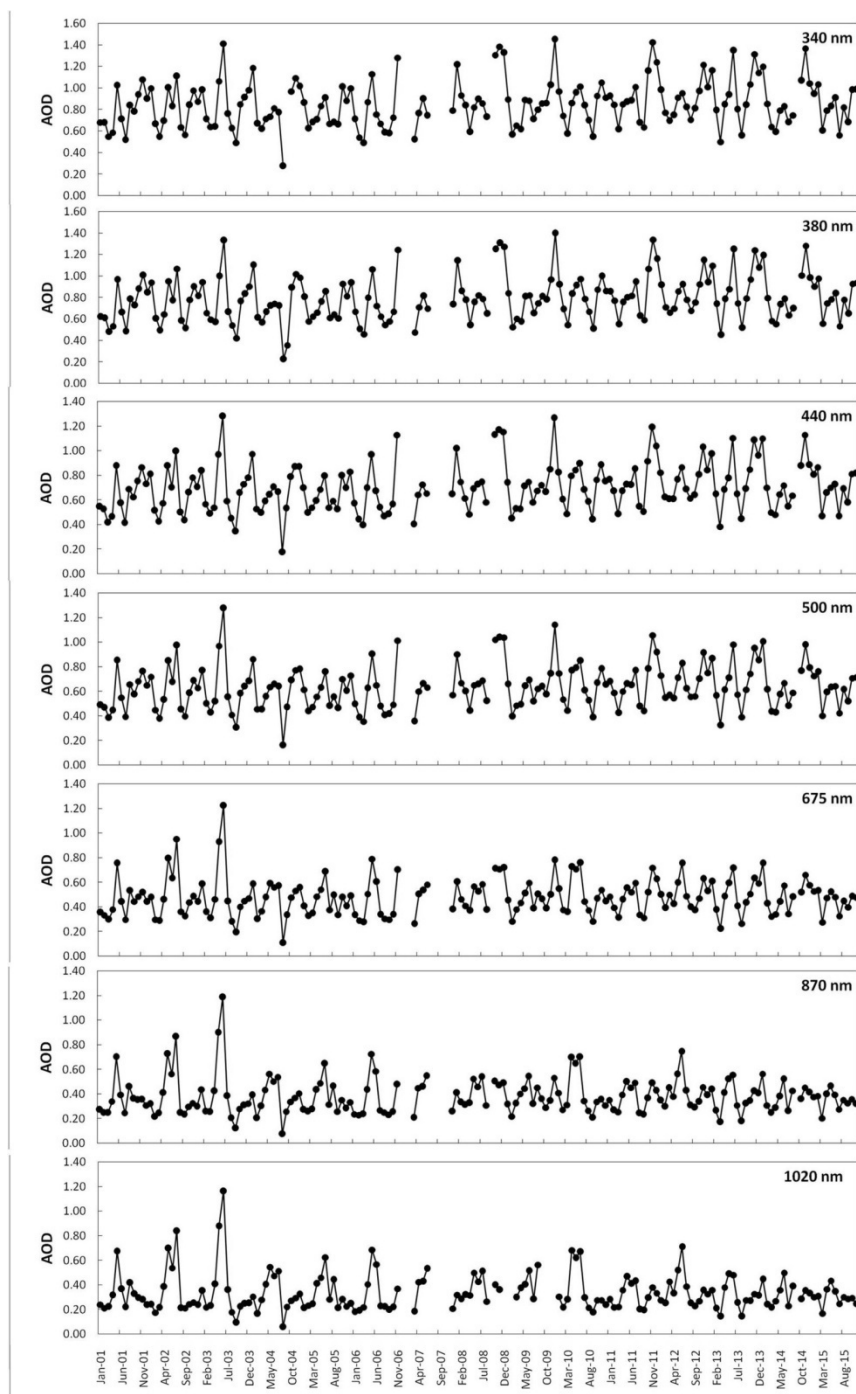


Fig 5. Month-wise variation in spectral AODs over the entire study period (period: January 2001 to November 2015).

The spectral variations show that in April- May, the AOD values are large at (340-380 nm) UV region, moderate at (440-675 nm) visible region of spectrum whereas smallest near (870-1020 nm) IR wavelength region.

Figure 6 shows the month wise variation in AOD at three representative wavelengths viz., 340nm, 500nm and 1025nm. The concept of choosing these wavelengths is to represent the ultraviolet, visible and near

infrared wavelength spectrum. With these wavelengths, one can estimate the aerosol size spectrum based on scattering variations with range radius $<0.1\mu\text{m}$ ⁽³⁾ because the effect of aerosol scattering can be easily assessed corresponding to these wavelengths⁽³⁾.

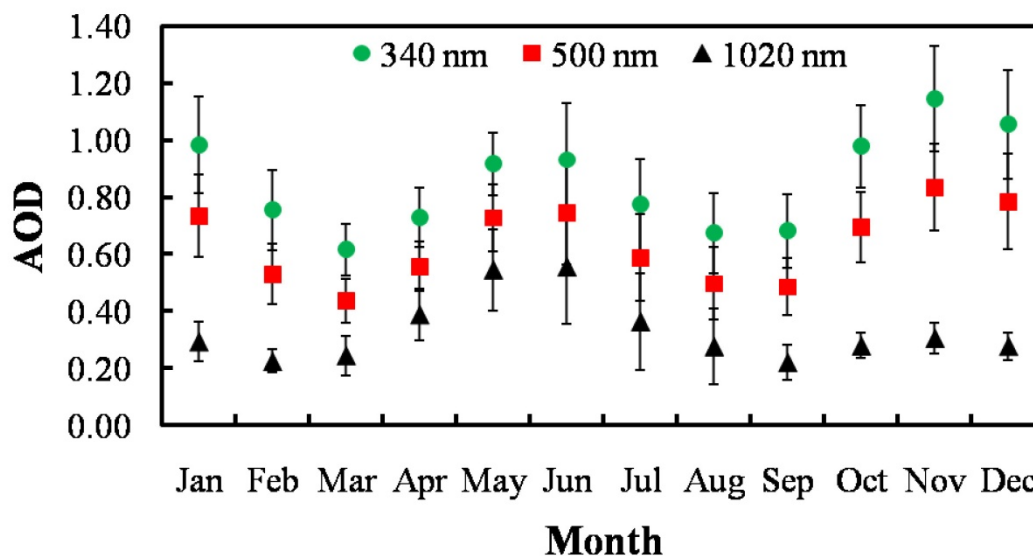


Fig 6. Variation in AOD at three representative wavelengths in different months of year during the period: 2001-2015

The AODs at shorter wavelengths may be due to fine mode aerosols, while at larger wavelengths may be attributed to coarse mode aerosols⁽³⁸⁾. Based on Kaskaoutis et al. (2013) study, we notice that there is hardly any variation in fine- mode radii; in contrast we notice an enhancement in coarse mode part⁽³⁹⁾. The results generalized that such restrictions are the properties of enhanced dust loading at larger AODs.

The vertical bars in [Figure 6](#) represent standard deviations. Remarkable variations (mean \pm standard deviation) at representative wavelengths for the entire duration indicated monthly averaged highest AOD values of 1.14 ± 0.18 at 340 nm and 0.83 ± 0.15 at 500 nm in November while 0.55 ± 0.20 at 1025 nm in June. The smallest AOD values recorded 0.61 ± 0.09 at 340 nm and 0.44 ± 0.09 at 500 nm in March while 0.22 ± 0.04 at 1025 nm in February. In entire period, the month wise mean AOD came out to 0.85 ± 0.16 , 0.63 ± 0.13 , 0.33 ± 0.11 at 340, 500 and 1025 nm respectively. The values of AOD ranged from 0.28 - 1.46, 0.17 - 1.28 and 0.18 - 1.54 at wavelengths 340, 500 and 1025 nm respectively.

4.3 Characteristics of spectral aerosol optical depth on the Basis of Season

The seasons in which average and standard deviation values of AOD for Kanpur site are classified like: pre-monsoon (March-May), monsoon (June-September), post-monsoon (October-November) and winter (December-February)⁽⁴⁰⁾. Black carbon contributes to AOD from 5 to 14% with relative contribution indicating very minor reduction with rising wavelengths whereas dust particles contributes to AOD greater than 55% (maxima) in the months May to June and less than 20% (minima) in November to January and thereby possesses an increasing trend with increasing wavelengths⁽⁴¹⁾. Depending on seasonal classification, average aerosol optical depths are approximated with standard deviation. The measured values of

AODs averaged over different seasons are shown in Figure 7 for seven CIMEL sun/sky spectral radiometer wavelengths.

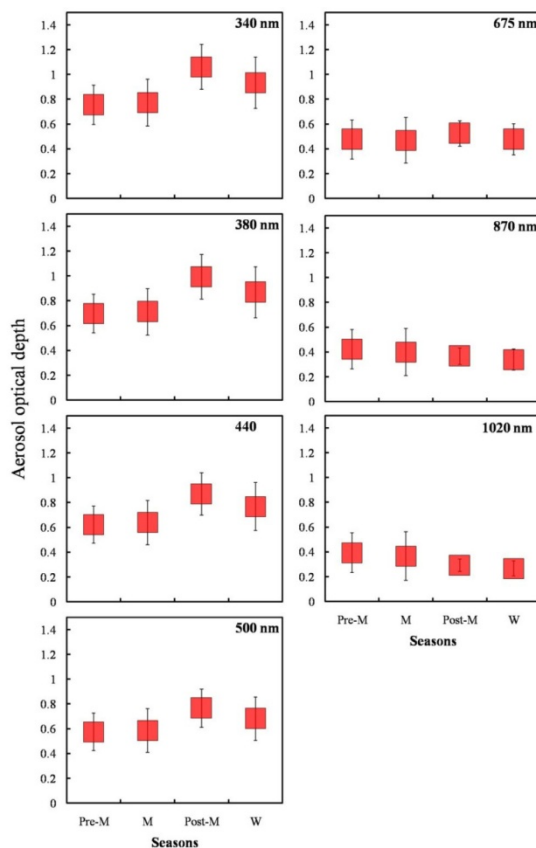


Fig 7. Seasonal characteristics of spectral aerosol optical depth averaged over different seasons namely: pre-monsoon (Pre-M), monsoon (M), post-monsoon (Post-M) and winter (W)

Post-monsoon season with reference to smaller wavelengths: the Figure 7 reveals that AOD attains maximum value in interval (λ :340-500 nm), less variation in interval (λ : 675-1020 nm), showing the pre-eminence of anthropogenic aerosols above the natural aerosols. At smaller wavelengths (λ : 340-500 nm), large values of standard deviation have been found which may be due to large variation in characteristics of spectral aerosol optical depth. Whereas at longer wavelength spectrum (λ : 675-1020 nm) standard deviation values are small, showing no significant variations in characteristics of spectral aerosol optical depth, especially in winter and post-monsoon seasons.

The sharp increase in AOD at shorter wavelengths shows that the fine aerosol particles concentration increases remarkably from pre-monsoon to post-monsoon seasons. The decrease in AOD at larger wavelengths represents that the concentration of coarse particles decreased during the same season. The post-monsoon (October-November) is followed by winter (December-February) 0.68 ± 0.18 , monsoon (June-September) 0.59 ± 0.18 and pre-monsoon (March-May) 0.57 ± 0.15 (refer to Figure 8).

The large value of AODs during post-monsoon and winter is attributed to high degree of anthropogenic emissions⁽⁴⁰⁾. In contrast, the small AOD values noticed during the periods of pre-monsoon and monsoon are chiefly impacted on by the variability of the dust outbursts⁽⁴⁰⁾. The AODs are large in winter season in the Indo- Gangetic Basin because of shallow boundary levels. The reasons for higher values of

AODs are due to the increased amount of bio fuels and fossil fuel, resulting foggy and hazy conditions⁽⁴²⁾. The AOD values lies between $0.40 < AOD \leq 0.70$ in months March to September, thereafter lies between $0.50 < AOD \leq 0.80$, no value of AOD lies below 0.30

Table 1. Frequency (%) distribution of AOD in different seasons.

| AOD | Pre-monsoon | Monsoon | Post-monsoon | Winter |
|------------------------|-------------|---------|--------------|--------|
| <0.10 | 0 | 0 | 0 | 0 |
| $0.10 < AOD \leq 0.20$ | 0 | 2 | 0 | 0 |
| $0.20 < AOD \leq 0.30$ | 0 | 0 | 0 | 0 |
| $0.30 < AOD \leq 0.40$ | 13 | 9 | 0 | 5 |
| $0.40 < AOD \leq 0.50$ | 24 | 22 | 3 | 17 |
| $0.50 < AOD \leq 0.60$ | 24 | 22 | 13 | 12 |
| $0.60 < AOD \leq 0.70$ | 20 | 33 | 31 | 22 |
| $0.70 < AOD \leq 0.80$ | 9 | 4 | 31 | 24 |
| $0.80 < AOD \leq 0.90$ | 4 | 3 | 0 | 10 |
| $0.90 < AOD \leq 1.0$ | 4 | 3 | 10 | 2 |
| >1.0 | 0 | 2 | 13 | 7 |

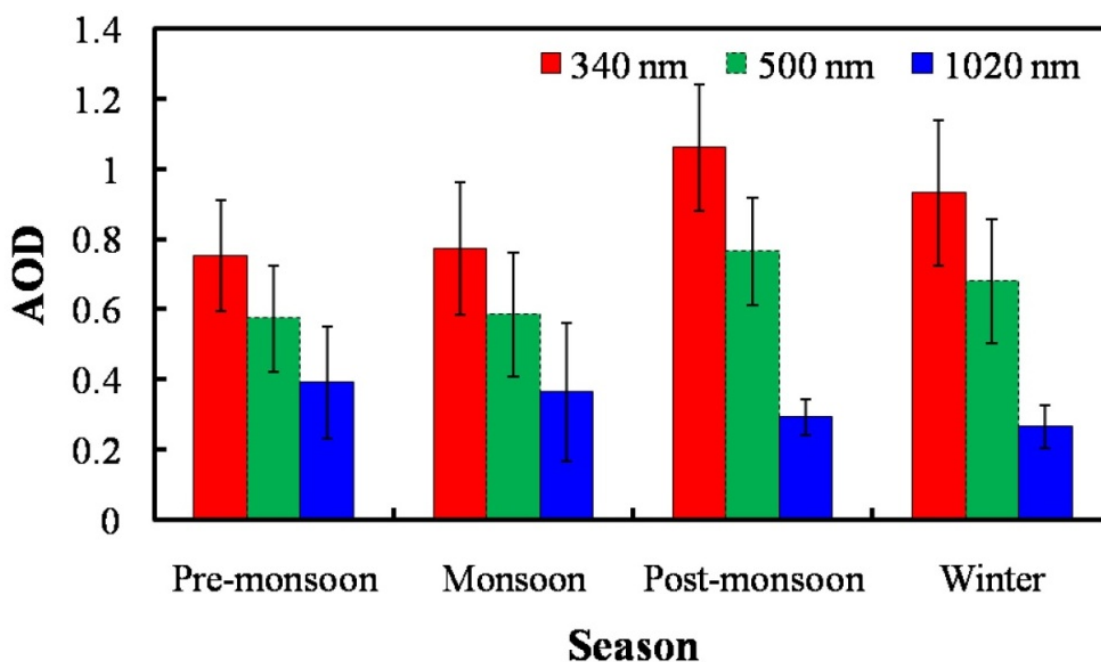


Fig 8. Solar Seasonal variation in AOD at 500 nm.

Figure 9 shows the histograms of AOD at 500 nm for all four seasons with average \pm standard deviation. The frequency distribution for the post monsoon has got narrow profile and ranges from 0.7 and 0.8, greater than 30% of the net month wise data in this bin. In winter the distribution widens and the maximum shifts to around 0.9. The distributions of pre-monsoon and monsoon are carried to smaller amounts of AOD.

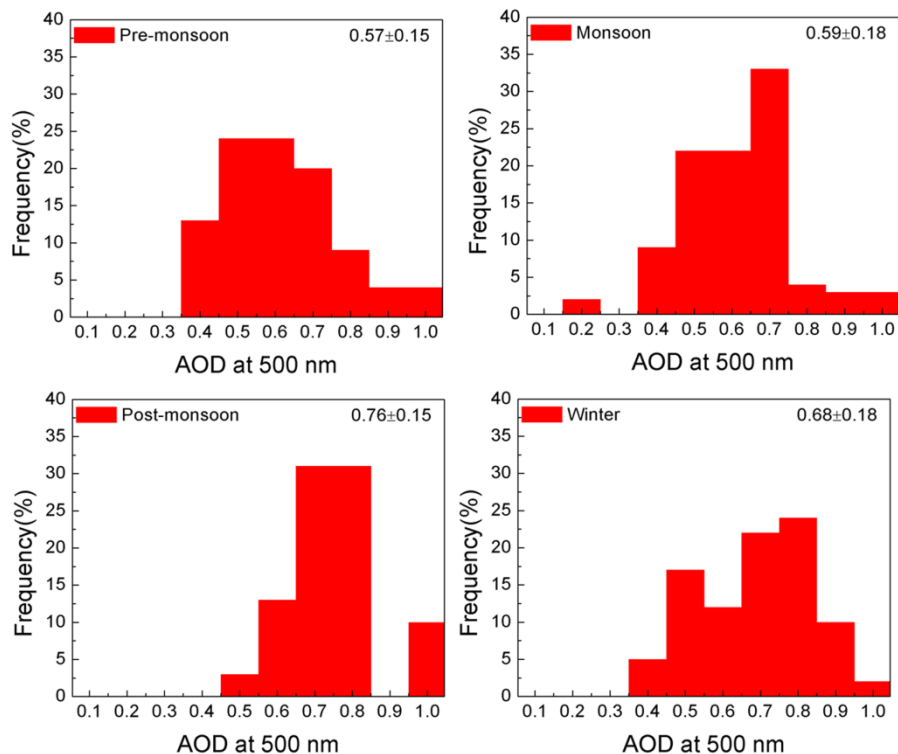


Fig 9. Seasonal frequency (%) histograms of AOD at 500 nm with mean \pm standard deviation, for the period averaged over: 2001-2015

4.4 Trend analysis

Figure 10 represents the linear trends in AOD at 500 nm (AOD_{500}). We used monthly averaged for the duration 2001–2015. In 2007, AOD data was not available for most of the months, possibly due to due to inclement weather or technical problems. Limited observations from June to September cause large variations from year to year due to the onset, intensity and duration of the monsoons⁽⁴³⁾. We conducted statistical studies taking into consideration the whole period (2001–2015), which also incorporates data gap. The slope, the intercepts on the Y – axis and coefficient of the determinants are given in Figure 10.

Inter-annual variability and trend of the AOD at 500 nm depending on monthly averaged observations over Kanpur for all data sets i.e., AERONET (upper panel), MODIS (middle panel), MISR (lower panel). The slope, Y-intercept and coefficient of determinants of the regression analysis are also mentioned in the figure.

The percentage change (%) of aerosol properties is calculated using the formula:

$$x(\%) = \frac{aN}{\bar{x}} \times 100$$

where x represents variable, a represents the slope of the linear regression fit and N the whole number of month⁽⁴⁰⁾. The variation in AERONET AOD per month, the difference in% and the statistical significance test are calculated by p-value. The AOD values show large monthly and seasonal variations in AOD_{500} for all datasets, such as AERONET, MODIS and MISR. The local and regional meteorological and weather conditions play a vital participation in modifying temporal variability in the AOD_{500} over different periods, especially in northern part of India⁽⁴⁴⁾. In India, the rainfall particularly in rainy season is main cause

of modulating aerosol properties^(43,45). In contrast, significant aerosol loading, particularly in northern India, can affect precipitation and the water cycle^(9,46).

Kaskaoutis et al. (2012), report that northern part is mainly influenced by mixed type of aerosols that includes local anthropogenic emission as well as desert dust, which are carried from western India. Consequently, the impact of rainfall in AOD trends over Kanpur is tough to quantify. For example, the lack in rainfall during the 2002 rainy season provided space for the loading of dust aerosols, which gave rise to high AOD values at the end of the pre-monsoon of 2003⁽⁴⁷⁾.

AERONET observations manifest consistent results. The increase in AERONET AOD₅₀₀ was statistically significant at the 95% confidence level ($p < 0.05$). Analysis of trends and percentage change (%) in the properties of aerosols are sensitive according to the averaged monthly observations⁽⁴⁰⁾. Therefore, the estimation of trend analysis based on averaged monthly observations has certain limitations, especially if there is a data gap. In such cases, observations may affect the averaged monthly values. Therefore, in this study, there may be biases in the trends.

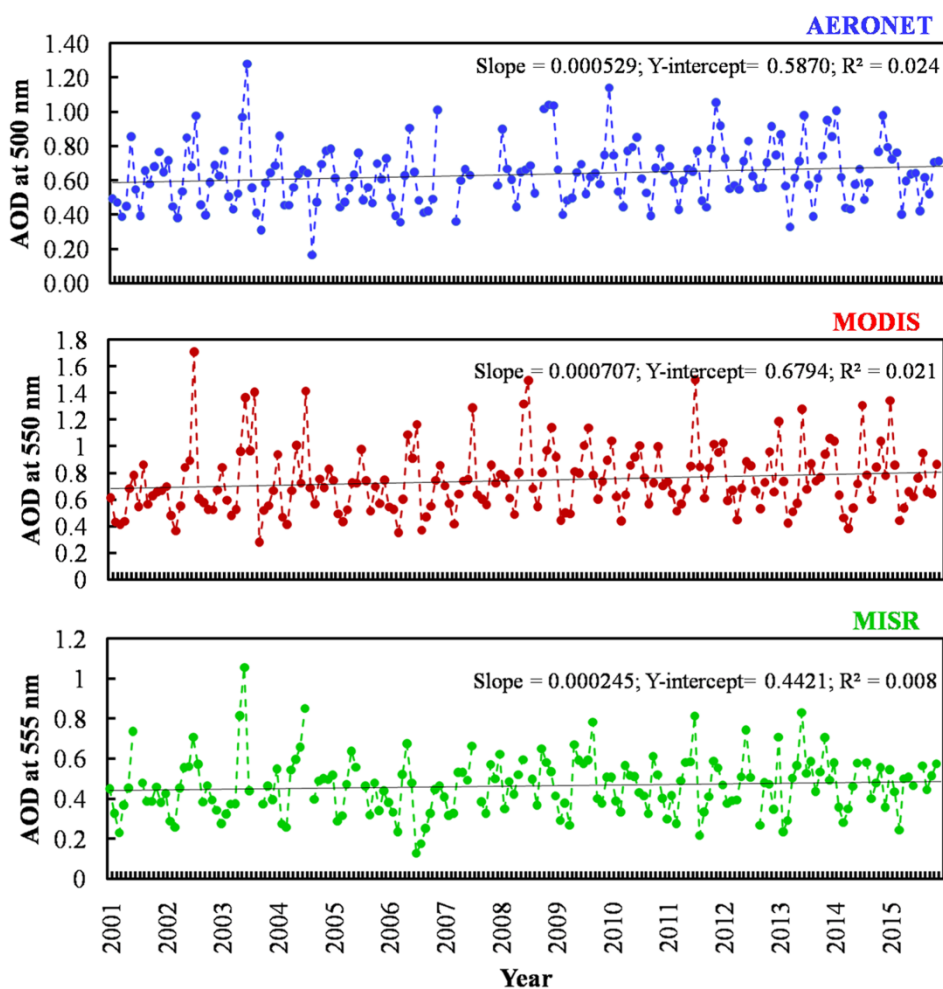


Fig 10. Inter-annual variability and trend of the AOD at 500 nm depending on monthly averaged observations over Kanpur for all data sets i.e., AERONET (upper panel), MODIS (middle panel), MISR (lower panel). The slope, Y-intercept and coefficient of determinants of the regression analysis are also mentioned in the figure

5 Conclusion

The optical properties of aerosols have distinct spectral and temporal variations depending upon the types and source of emissions over Kanpur region. The work investigated the spectral and seasonal variations of AOD over Kanpur region (IGP) using AERONET data for the period 2001 -2015. The main points of the conclusions of this study are:

1. The AOD at 340 nm and 500 nm consistently increased with effect from pre-monsoon (March-May) to post-monsoon (October-November) with values 41% and 33% respectively because mostly the weather remains raining and cloudy in this period and effects the measurements. On the other hand at 1020 nm, there is the reduction in AOD having approximate value of 26%. The largest AOD at 500 nm record in post-monsoon is 0.76 ± 0.15 .

2. At shorter wavelengths (340-500 nm), there is sharp increase in AOD whereas at longer wavelengths (675-1020 nm), decrease in AOD has been noticed. The large standard deviations of AODs indicated higher month-to-month changes in the features of aerosols.

3. Kanpur recorded overall an growing trends in AERONET AOD₅₀₀ (14%), which found in good agreement with Moderate Resolution Imaging Spectroradiometer (MODIS) . All data sets showed a consistent increase in AOD at 500 nm, which indicates that the emission of anthropogenic aerosols continuously increasing over Kanpur. However trends in MODIS AOD₅₀₀ and MISR AOD₅₀₀ are not statistically significant at the 95% confidence level. The trend obtained from MODIS having no data-gap, found consistence with AERONET and MISR observations, suggests that the all datasets deployed for the trend analysis are reliable despite the lack of data during some months.

Acknowledgments

The authors heartily thank Dean (Research and Higher Studies), Career Point University, Kota for their kind cooperation and extended support. We accept with great gratitude the distinguished jobs and sources of data like CIMEL sun photometer that have been utilized and ascribed in the paper in direct or indirect way.

References

- 1) Meszaros E. Atmospheric chemistry fundamental aspects. New York. Elsevier Scientific Publishing Company. 1981. Available from: <https://www.elsevier.com/books/atmospheric-chemistry/meszaros/978-0-444-99753-1>.
- 2) Eck TF, Holben BN, Reid JS, Dubovik O, Smirnov A, O'Neill NT, et al. Wavelength dependence of the optical depth of biomass burning, urban, and desert dust aerosols. *Journal of Geophysical Research: Atmospheres*. 1999;104(D24):31333–31349. Available from: <https://dx.doi.org/10.1029/1999jd900923>.
- 3) Schuster GL, Dubovik O, Holben BN. Ångström exponent and bimodal aerosol size distributions. *Journal of Geophysical Research*. 2006;111:1–14. Available from: <https://doi.org/10.1029/2005JD006328>.
- 4) Pósfai M, Buseck PR. Nature and Climate Effects of Individual Tropospheric Aerosol Particles. *Annual Review of Earth and Planetary Sciences*. 2010;38(1):17–43. Available from: <https://dx.doi.org/10.1146/annurev.earth.031208.100032>.
- 5) Junge CE. Air chemistry and radioactivity. New York. Academic Press. 1963.
- 6) Pöschl U. Atmospheric Aerosols: Composition, Transformation, Climate and Health Effects. *Angewandte Chemie International Edition*. 2005;44(46):7520–7540. Available from: <https://dx.doi.org/10.1002/anie.200501122>.
- 7) Charlson RJ, Schwartz SE, Hales JM, Cess RD, Coakley JA, Hansen JE, et al. Climate Forcing by Anthropogenic Aerosols. *Science*. 1992;255(5043):423–430. Available from: <https://dx.doi.org/10.1126/science.255.5043.423>.
- 8) Gray V. The Physical Science Basis. Cambridge University Press. 2007. Available from: <https://doi.org/10.1260/095830507781076194>.
- 9) Ramanathan V, Chung C, Kim D, Bettge T, Buja L, Kiehl JT, et al. Atmospheric brown clouds: Impacts on South Asian climate and hydrological cycle. *Proceedings of the National Academy of Sciences*. 2005;102(15):5326–5333. Available from:

- <https://dx.doi.org/10.1073/pnas.0500656102>.
- 10) Vinoj V, Rasch PJ, Wang H, Yoon JH, Ma PL, Landu K, et al. Short-term modulation of Indian summer monsoon rainfall by West Asian dust. *Nature Geoscience*. 2014;7(4):308–313. Available from: <https://dx.doi.org/10.1038/ngeo2107>.
 - 11) Dockery DW, Pope CA, Xu X, Spengler JD, Ware JH, Fay ME, et al. An Association between Air Pollution and Mortality in Six U.S. Cities. *New England Journal of Medicine*. 1993;329(24):1753–1759. Available from: <https://dx.doi.org/10.1056/nejm199312093292401>.
 - 12) on Climate Change IGP. Summary for Policymakers. In Climate Change 2013 – The Physical Science Basis. Cambridge University Press. 2013. Available from: <https://doi.org/10.1017/CBO9781107415324.004>.
 - 13) Prospero JM, Ginoux P, Torres O, Nicholson SE, Gill TE. Environmental characterization of global sources of atmospheric soil dust identified with the Nimbus. *Reviews of Geophysics*. 2002;40(1). Available from: <https://doi.org/10.1029/2000RG000095>.
 - 14) Kedia S, Ramachandran S. Variability in aerosol optical and physical characteristics over the Bay of Bengal and the Arabian Sea deduced from Ångström exponents. *Journal of Geophysical Research*. 2009;114(D14):1–13. Available from: <https://dx.doi.org/10.1029/2009jd011950>.
 - 15) Kedia S, Ramachandran S, Kumar A, Sarin MM. Spatiotemporal gradients in aerosol radiative forcing and heating rate over Bay of Bengal and Arabian Sea derived on the basis of optical, physical, and chemical properties. *Journal of Geophysical Research*. 2010;115(D7):1–17. Available from: <https://dx.doi.org/10.1029/2009jd013136>.
 - 16) Prospero JM. African Droughts and Dust Transport to the Caribbean: Climate Change Implications. *Science*. 2003;302(5647):1024–1027. Available from: <https://dx.doi.org/10.1126/science.1089915>.
 - 17) Singh RP, Dey S, Tripathi SN, Tare V, Holben B. Variability of aerosol parameters over Kanpur, northern India. *Journal of Geophysical Research: Atmospheres*. 2004;109(D23). Available from: <https://dx.doi.org/10.1029/2004jd004966>.
 - 18) Kaskaoutis DG, Badarinath KVS, Kharol SK, Sharma AR, Kambezidis HD. Variations in the aerosol optical properties and types over the tropical urban site of Hyderabad, India. *Journal of Geophysical Research*. 2009;114(D22). Available from: <https://dx.doi.org/10.1029/2009jd012423>.
 - 19) Guleria RP, Kuniyal JC. Characteristics of atmospheric aerosol particles and their role in aerosol radiative forcing over the northwestern Indian Himalaya in particular and over India in general. *Air Quality, Atmosphere & Health*. 2016;9(7):795–808. Available from: <https://dx.doi.org/10.1007/s11869-015-0381-0>.
 - 20) Gueymard C, Rejomon G. Gridded aerosol data for improved direct normal irradiance modeling: The case of India. In: and others, editor. 40th ASES National Solar Conference 2011, SOLAR 2011. 2011. Available from: <https://www.nrel.gov/docs/fy14osti/61121.pdf>.
 - 21) Srivastava A, Tiwari S, Devara P, Bisht D, Srivastava M, Tripathi S, et al. Pre-monsoon aerosol characteristics over the Indo-Gangetic Basin: Implications to climatic impact. *Annales Geophysicae*. 2011;29:789–804. Available from: <https://doi.org/10.5194/angeo-29-789-2011>.
 - 22) Sarangi C, Tripathi SN, Mishra AK, Goel A, Welton EJ. Elevated aerosol layers and their radiative impact over Kanpur during monsoon onset period. *Journal of Geophysical Research: Atmospheres*. 2016;121(13):7936–7957. Available from: <https://dx.doi.org/10.1002/2015jd024711>.
 - 23) Sharma M, Kiran YNVM, Shandilya KK. Investigations into formation of atmospheric sulfate under high PM10 concentration. *Atmospheric Environment*. 2003;37(14):2005–2013. Available from: [https://dx.doi.org/10.1016/s1352-2310\(03\)00005-0](https://dx.doi.org/10.1016/s1352-2310(03)00005-0).
 - 24) Tripathi SN, Dey S, Tare V, Satheesh SK, Lal S, Venkataramani S. Enhanced layer of black carbon in a north Indian industrial city. *Geophysical Research Letters*. 2005;32(12). Available from: <https://dx.doi.org/10.1029/2005gl022564>.
 - 25) Shrestha S, Peel M, Moore G. Development of a Regression Model for Estimating Daily Radiative Forcing Due to Atmospheric Aerosols from Moderate Resolution Imaging Spectrometers (MODIS) Data in the Indo Gangetic Plain (IGP). *Atmosphere*. 2018;9:405–405. Available from: <https://dx.doi.org/10.3390/atmos9100405>.
 - 26) Holben BN. AERONET- a federated instrument network and data archive for aerosol characterization. *Remote Sensing of Environment*. 1998;66:1–16. Available from: <https://doi.org/10.3390/atmos9100405>.
 - 27) Iqbal M. An introduction to solar radiation; vol. 390. London. Academic Press. 1983. Available from: <https://www.elsevier.com/books/an-introduction-to-solar-radiation/iqbal/978-0-12-373750-2>.
 - 28) Shaw GE, Reagan JA, Herman BM. Investigations of Atmospheric Extinction Using Direct Solar Radiation Measurements Made with a Multiple Wavelength Radiometer. *Journal of Applied Meteorology*. 1973;12(2):374–380. Available from: [https://dx.doi.org/10.1175/1520-0450\(1973\)012<0374:ioaeud>2.0.co;2](https://dx.doi.org/10.1175/1520-0450(1973)012<0374:ioaeud>2.0.co;2).
 - 29) Dubovik O, King MD. A flexible inversion algorithm for retrieval of aerosol optical properties from Sun and sky radiance measurements. *Journal of Geophysical Research: Atmospheres*. 2000;105(D16):20673–20696. Available from: <https://dx.doi.org/10.1029/1999jd000235>.

[org/10.1029/2000jd900282](https://doi.org/10.1029/2000jd900282).

- 30) Mishchenko MI, Travis LD, Lacis AA. Scattering absorption, and emission of light by small particles. New York. Cambridge University Press. 2002. Available from: <https://www.giss.nasa.gov/staff/mmishchenko/books.html>.
- 31) Dubovik O, Sinyuk A, Lapyonok T, Holben BN, Mishchenko M, Yang P, et al. Application of spheroid models to account for aerosol particle nonsphericity in remote sensing of desert dust. *Journal of Geophysical Research*. 2006;111(D11):D11208. Available from: <https://dx.doi.org/10.1029/2005jd006619>. doi:10.1029/2005jd006619.
- 32) Dubovik O, Holben B, Eck TF, Smirnov A, Kaufman YJ, King MD. Variability of Absorption and Optical Properties of Key Aerosol Types Observed in Worldwide Locations. *Journal of the Atmospheric Sciences*. 2002;59(3):590–608. Available from: [https://dx.doi.org/10.1175/1520-0469\(2002\)059<0590:voaaop>2.0.co;2](https://dx.doi.org/10.1175/1520-0469(2002)059<0590:voaaop>2.0.co;2).
- 33) Cachorro VE, Durán P, Vergaz R, de Frutos AM. Measurements of the atmospheric turbidity of the North-centre continental area in Spain: spectral aerosol optical depth and Ångström turbidity parameters. *Journal of Aerosol Science*. 2000;31(6):687–702. Available from: [https://dx.doi.org/10.1016/s0021-8502\(99\)00552-2](https://dx.doi.org/10.1016/s0021-8502(99)00552-2).
- 34) Gueymard CA. The sun's total and spectral irradiance for solar energy applications and solar radiation models. *Solar Energy*. 2004;76(4):423–453. Available from: <https://dx.doi.org/10.1016/j.solener.2003.08.039>.
- 35) Eck TF, Holben BN, Ward DE, Dubovik O, Reid JS, Smirnov A. Characterization of the optical properties of biomass burning aerosols in Zambia during the 1997 ZIBBEE field campaign. *Journal of Geophysical Research: Atmospheres*. 2001;106(D4):3425–3448. Available from: <https://dx.doi.org/10.1029/2000jd900555>.
- 36) Bibi H, Alam K, Blaschke T, Bibi S, Iqbal MJ. Long-term (2007–2013) analysis of aerosol optical properties over four locations in the Indo-Gangetic plains. *Applied Optics*. 2016;55(23):6199–6199. Available from: <https://dx.doi.org/10.1364/ao.55.006199>. doi:10.1364/ao.55.006199.
- 37) Kumar KR, Narasimhulu K, Reddy RR, Gopal KR, Reddy LSS, Balakrishnaiah G. Temporal and spectral characteristics of aerosol optical depths in a semi-arid region of southern India. *Science of The Total Environment*. 2009;407(8):2673–2688. Available from: <https://dx.doi.org/10.1016/j.scitotenv.2008.10.028>.
- 38) Kedia S, Ramachandran S. Seasonal variations in aerosol characteristics over an urban location and a remote site in western India. *Atmospheric Environment*. 2011;45(12):2120–2128. Available from: <https://dx.doi.org/10.1016/j.atmosenv.2011.01.040>.
- 39) Kaskaoutis DG, Sinha PR, Vinoj V, Kosmopoulos PG, Tripathi SN, Misra A. Aerosol properties and radiative forcing over Kanpur during severe aerosol loading conditions. *Atmospheric Environment*. 2013;79:7–19. Available from: <https://dx.doi.org/10.1016/j.atmosenv.2013.06.020>.
- 40) Kaskaoutis DG, Singh RP, Gautam R, Sharma M, Kosmopoulos PG, Tripathi SN. Variability and trends of aerosol properties over Kanpur, northern India using AERONET data (2001–10). *Environmental Research Letters*. 2012;7(2):024003–024003. Available from: <https://dx.doi.org/10.1088/1748-9326/7/2/024003>.
- 41) Dey S, Sn. Aerosol direct radiative effects over Kanpur in the Indo-Gangetic basin, northern India: Long-term (2001–2005) observations and implications to regional climate. *Journal of Geophysical Research*. 2013;(D4):113–113.
- 42) Ramachandran S, Kedia S. Aerosol Optical Properties over South Asia from Ground-Based Observations and Remote Sensing: A Review. *Climate*. 2013;1:84–119. Available from: <https://dx.doi.org/10.3390/cli1030084>.
- 43) Gautam R, Hsu NC, Lau KM, Kafatos M. Aerosol and rainfall variability over the Indian monsoon region: distributions, trends and coupling. *Annales Geophysicae*. 2009;27(9):3691–3703. Available from: <https://dx.doi.org/10.5194/angeo-27-3691-2009>.
- 44) Singh RP, Dey S, Tripathi SN, Tare V, Holben B. Variability of aerosol parameters over Kanpur, northern India. *Journal of Geophysical Research: Atmospheres*. 2004;109(D23):1–14. Available from: <https://dx.doi.org/10.1029/2004jd004966>.
- 45) Manoj MG, Devara PCS, Safai PD, Goswami BN. Absorbing aerosols facilitate transition of Indian monsoon breaks to active spells. *Climate Dynamics*. 2011;37(11–12):2181–2198. Available from: <https://dx.doi.org/10.1007/s00382-010-0971-3>.
- 46) Lau KM, Kim KM. Observational relationships between aerosol and Asian monsoon rainfall, and circulation. *Geophysical Research Letters*. 2006;33(21):1–5. Available from: <https://dx.doi.org/10.1029/2006gl027546>.
- 47) Kaskaoutis DG, Kharol SK, Sinha PR, Singh RP, Badarinath KVS, Mehdi W. Contrasting aerosol trends over South Asia during the last decade based on MODIS observations. *Atmospheric Measurement Techniques Discussions*. 2011;4(4):5275–5323. Available from: <https://dx.doi.org/10.5194/amtd-4-5275-2011>.